Dynamic Viscoelastic Characterization of Sol–Gel Reactions

Donald F. Hodgson and Eric J. Amis*

Department of Chemistry, University of Southern California, Los Angeles, California 90089-0482. *Received October 2, 1989; Revised Manuscript Received November 27, 1989*

ABSTRACT: The evolution of viscoelasticity in a tetraethoxysilane gel system has been measured starting immediately following mixing and proceeding through the macroscopic gel point. The storage and loss dynamic shear moduli, $G'(\omega)$ and $G''(\omega)$, were determined with the multiple-lumped resonator instrument as a function of time for frequencies in the range 104–6200 Hz. The water to silane monomer ratio maintained at 6:1, while the concentration of HCl acid catalyst was varied in separate measurements. The scaling exponent for the variation of G' and G'' with frequency at the gel point is $\Delta = 0.72 \pm 0.02$. Reaction time dependent shift factors for the frequency and modulus are determined which allow creation of a modulus–frequency master curve. The scaling of these shift factors with the extent of reaction yields critical exponents for zero shear viscosity, elastic modulus, and cluster radius.

Introduction

Due to the importance of gelation phenomena in current technologies and as a model system for exploring the nature of critical points, increasingly sophisticated experiments and theories have been developed. From the original mean-field theories of Flory[1] and Stockmayer,[2] current emphasis has shifted to the utilization of the concepts of fractal geometry[3–6] and the connectivity transition model of percolation.[7,8] Under the percolation model, predictions for numerous physical properties are made when the gelation reaction bath is considered a polydisperse self-similar distribution of polymeric clusters (fractals), which grow from the initiation of the reaction on through the gel point. In the past few years there have also been several experimental studies performed on a diverse range of polymeric systems that seek to test the validity of the theoretical models. Static properties of gelation reaction systems have been examined with small-angle X-ray,[9,10] neutron[11] and light scattering techniques,[12–14] and also by chromatographic analysis.[14] Dynamical properties have been studied by dynamic light scattering[15] and rheological measurements.[6,16–19] Recently focus has been placed on viscoelasticity as a direct probe of the change from liquidlike to solidlike behavior during the sol to gel transition.[4,6,17,19] To describe the time evolution of viscoelastic properties throughout a gelation reaction is the purpose of this study.

Several different chemical systems have been used for studies of gelation reactions and as models of gels with specific structures and properties. One system that has received considerable recent attention is the gelation of alkoxysilanes. These glass-forming gels have applications for a variety of optical and structural materials.[10,20] In aqueous solution alkoxysilicates undergo a hydrolysis reaction, followed by condensation and eventual gelation. The type of catalyst and the relative reactant ratios yield gels of varying microscopic and macroscopic properties.[10,21] The ability to change the nature of the gel based on readily adjustable parameters makes these silicate systems particularly attractive in testing the model predictions and their universality.

The Flory–Stockmayer (FS) mean field theory and the percolation models both provide scaling relations for the divergence of static properties of the polymeric species at the gelation threshold. The correlation length in the reaction bath is defined by the z-average cluster radius of gyration, which scales with the extent of reaction p as

$$R_z \sim \left(\frac{|p - p_c|}{p_c}\right)^{-\nu} \quad \text{for } p < p_c \tag{1}$$

where p_c is the extent of reaction at the sol–gel transition critical point. The weight average molecular weight of a cluster in solution diverges as

$$M_w \sim \left(\frac{|p - p_c|}{p_c}\right)^{-\gamma} \quad \text{for } p < p_c \tag{2}$$

For FS theory the predicted exponents are $\gamma = 1$ and $\nu = {}^1/_2$, while for percolation they are calculated as 1.76 and 0.88, respectively.[7] Correlation lengths R_z and cluster masses M_w can be determined by size-exclusion chromatography and/or static light scattering. The exponents obtained depend on the type of polymer system studied, where reported values are $\gamma = 1.65 \pm 0.1$ and $\nu = 0.86 \pm 0.1$ for a polyurethane[22] and $\gamma = 1.8 \pm 0.3$ and $\nu = 1.1 \pm 0.2$ for a polyester.[14]

Scaling predictions for the steady-state viscoelastic properties have also been developed in both theories. The growth of the equilibrium modulus after the critical point can be described as a function of p by

$$G_0 \sim \left(\frac{|p - p_c|}{p_c}\right)^{t} \quad \text{for } p > p_c \tag{3}$$

and similarly the zero shear rate viscosity as

$$\eta_0 \sim \left(\frac{|p - p_c|}{p_c}\right)^{-s} \quad \text{for } p < p_c \tag{4}$$

For FS theory the predicted modulus scaling exponent is $t = 3$, while the viscosity is not predicted to diverge, growing only logarithmically ($s = 0$) near the gel point. Calculations based on Rouse-like dynamics for percolation clusters in the reaction bath[4,19] give $t = 2.67$ and $s = 1.33$. Calculations of an elastic network provide the predicted scaling exponent[24] $t = 3.96 \pm 0.04$, while $s = 0.75 \pm 0.04$ for analogy of the gelation phenomenon to a percolation model of superconductor–resistor networks.[8,23,25] Experimentally, exponent values have been obtained from measured values of the shear modulus and viscosity at small, but finite, shear rates. Values range from $t = 3.2 \pm 0.6$ and $s = 0.8 \pm 0.1$ for condensation polymerizations of polyols and diisocyanates,[16] $s = 1.4 \pm 0.2$ for epoxy resin systems,[18] and $t = 3.6 \pm 0.4$ and $s = 1.1 \pm 0.3$ for tetraethoxysilane.[26] Some workers ques-

* To whom correspondence should be addressed.

0024-9297/90/2223-2512$02.50/0

tion the rigor of applying zero shear predictions to measurements which have been performed at low, but nonzero, shear rates.[19]

Consideration of the dynamics near the gelation critical point has led to predictions for the frequency dependence of the components of the complex shear modulus $G^*(\omega) = G'(\omega) + iG''(\omega)$, where $G'(\omega)$ and $G''(\omega)$ are the storage and loss shear moduli, respectively. At the gel point they are observed[36,37] and predicted[4,6,19] to scale with frequency as $G' \sim G'' \sim \omega^{\Delta}$. To determine Δ, the various models treat the gelation reaction bath as a polydisperse ensemble composed of polymer fractals, objects which are self-similar on all length scales and having masses scaling as $M \sim R^{d_f}$. These clusters are treated in the Rouse limit as free draining (hydrodynamically noninteracting) with relaxation times proportional to mass, $\tau_i \sim M_i$ between some minimum and maximum cutoffs.[4,19] The minimum is defined by the molecular weight between crosslinks, M_x, while the maximum cutoff is the mass of a cluster whose radius is R_z (the correlation length). The inclusion of a high molecular weight cutoff eliminates the problem of the size divergence of the largest cluster as the gel point is approached, while the lower cutoff results from the lack of self-similarity on very small distance scales. The environment of any test molecule of mass M' is composed of smaller fractal clusters which relax at a faster rate, $\tau_i < \tau'$, and larger clusters which are considered immobile on the test molecule time scale. Clusters of dimensions greater than R_z feel the bulk viscosity of the solution. Under this description of the dynamics, the shear modulus is given by

$$G(\tau) \sim 1/\tau^{\Delta} \tag{5}$$

where $\Delta = t/(s + t)$. On Fourier transformation the frequency dependence of the modulus is observed as

$$G(\omega) \sim \omega^{\Delta} \tag{6}$$

This gives the prediction of $\Delta = 0.67$ at the gel point using the zero frequency values for s and t. Use of the values for s and t calculated from analogy to resistor–superconductor networks gives $\Delta = 0.72 \pm 0.2$. Experimentally, the observed scaling at the gel point is $\Delta = 0.70 \pm 0.05$ for epoxy resins,[18] 0.69 ± 0.02 for polyurethanes,[17] 0.69 ± 0.02 for polyesters,[19] and 0.5–0.7 for PDMS[37] and polyurethanes.

The predictions for the dynamics at the gel point and the theory of viscoelasticity can be used to obtain values for the static scaling exponents. The zero shear viscosity is determined by the arithmetic average relaxation time, which is given by the time integral of the shear relaxation modulus[27]

$$\langle\tau\rangle \equiv \int_0^{\infty} G(\tau)\, d\tau \sim \left(\frac{|p - p_c|}{p_c}\right)^{-s} \tag{7}$$

The longest (terminal) relaxation time in the neighborhood of the gel point is given by τ_z, which has been shown[4] to diverge as

$$\tau_z \equiv \frac{\int_0^{\infty} \tau G(\tau)\, d\tau}{\int_0^{\infty} G(\tau)\, d\tau} \sim \left(\frac{|p - p_c|}{p_c}\right)^{-s-t} \tag{8}$$

where it is noted that $\tau_z \sim \eta_0 J_e^0$, the product of the zero shear viscosity and the steady-state creep compliance.[27] Since $\langle\tau\rangle \sim \eta_0$, eqs 7 and 8 lead to

$$\frac{1}{J_e^0} \sim \frac{\langle\tau\rangle}{\tau_z} \sim \left(\frac{|p - p_c|}{p_c}\right)^{t} \tag{9}$$

The use of these two divergent time scales has led to the identification[4] of the zero shear modulus exponent t as $d\nu$, where d is the spatial dimension, and therefore $\Delta = d\nu/(s + d\nu)$.

The divergence of the terminal relaxation time τ_z is significant since it indicates that a *fixed* observational frequency is shifted to higher *effective* frequencies as a gelation reaction evolves. Therefore an experiment can be performed at one frequency, and, as the reaction progresses as a function of time from initiation up to the gel point, $G'(\omega)$ can be scaled by the equilibrium modulus G_0 and ω by the longest relaxation time τ_z. Before the gel point G_0 is given by $1/J_e^0$ allowing the complex modulus to be scaled by the steady state shear compliance. This results in the creation of a viscoelastic master curve of GJ_e^0 plotted against $\omega\tau_z$, with increasing values on the frequency and modulus axes corresponding to longer reaction times (closer to the gel point).

This paper describes the measurement of the frequency-dependent viscoelasticity of a series of tetraethoxysilane gelation reactions using a multiple-lumped resonator (MLR) instrument.[28] The MLR, a device originally constructed for the determination of intrinsic dynamic storage and loss shear moduli from dilute polymer solutions,[27-30] was used to measure the time evolution of viscoelasticity for gelation reactions from initiation through the gel point. Using the MLR we are able to directly determine $G'(\omega)$ and $G''(\omega)$ and also the scaling exponent Δ at the gel point for each reaction. Time-dependent shift factors are calculated and the critical point exponents s, t, and ν are examined.

Experimental Section

The gelation reactions under investigation are the acid-catalyzed hydrolysis and condensation of tetraethoxysilane (TEOS)

$$Si(OEt)_4 + H_2O \xrightarrow{H^+} Si(OEt)_3OH + EtOH$$

$$2Si(OEt)_3OH \rightarrow (EtO)_3SiOSi(OEt)_3 + H_2O$$

where the reaction bath contains TEOS, ethanol, and H_2O with added HCl. A series of three gels were prepared with a constant water to monomer mole ratio of 6.19:1, each catalyzed by a varying concentration of HCl, with the pH ranging from 3.1 to 4.4. The complete polymerization process is not yet understood. It was originally suggested that low pH and low water conditions favor gel networks composed of predominantly linear polymer chains with light cross-linking.[9,10] Gels formed under more basic conditions (pH > 4) and with large water to silicate ratios produce gels composed of highly branched (cross-linked) colloidal polymeric clusters.[31] On the other hand, it has been suggested that a transition occurs from cluster–cluster growth at low pH to monomer–cluster growth at high pH leading to a change from branched polymers to colloidal particles.[32] Thus at very high pH silica particles are formed, followed by aggregation and eventual coagulation. For the study reported here the pH and high water to monomer ratio favors production of a gel composed of highly branched polymer clusters. Cryogenic transition electron microscopy has demonstrated that the structural differences between high and low pH gels persist up to distance scales over 100 nm.[33]

Tetraethoxysilane (Aldrich Chemical Co.) was distilled under reduced pressure prior to use. Absolute ethyl alcohol was obtained fresh and used without further purification. Distilled and deionized water was used in the preparation of each HCl solution. The reaction mixture was prepared by dropwise addition of one part aqueous HCl to a premixed solution of two parts each of TEOS and alcohol. A solution of 1.8 M TEOS was thus produced. Each HCl solution was prepared separately to give a reaction bath solution the appropriate acidity. All reagents were equilibrated at 30 °C prior to mixing. Exothermic monomer hydrolysis occurs during the initial mixing period, with higher

Table I
Values Obtained for the Gel Point, Crossover Frequency, and Scaling Exponents for Solutions with Different Reaction Acidities

pH	t_g, s	t, s ($G' = G''$)	Δ	s	t	ν	$\Delta\ (t/[s+t])$
3.1	560 000	625 000	0.70 ± 0.02	$0.9_5 \pm 0.1$	2.4 ± 0.2	0.80 ± 0.07	$0.7_2 \pm 0.1$
3.4	350 000	375 000	0.72 ± 0.02	$0.8_8 \pm 0.2$	2.2 ± 0.3	0.73 ± 0.09	$0.7_1 \pm 0.1$
4.4	86 000	95 000	0.71 ± 0.03	$0.7_9 \pm 0.3$	2.6 ± 0.3	0.87 ± 0.09	$0.7_7 \pm 0.1$

acidities producing demonstratably more heat. After starting as nonhomogeneous and opaque two-phase systems, continual vigorous stirring results in clear single-phase solutions that are subsequently used for the viscoelastic experiments. Typically, higher acidities result in a more rapid clarification. It has been previously noted that at the onset of the reaction the ethanol present may not completely cosolubilize the TEOS and water.[11] Therefore, until enough ethoxy groups have been converted into silanols the hydrolysis occurs at the TEOS/water interface. The rates of condensation, branching, and hydrolysis have each been shown to be pH-dependent.

Measurement of the dynamic VE properties of the TEOS solution during the sol–gel transition was performed by using the multiple-lumped resonator (MLR) instrument constructed in our laboratory.[28,30] The MLR determines G' and G'' over a laboratory frequency range of 104–6200 Hz. The basic element of the MLR is a mechanical resonator, machined from a single titanium rod, suspended in a precision-bore Pyrex tube that serves as the sample cell for the solution under investigation. The resonator consists of five identical fat segments (lumps) connected and held by six thin segments of varying diameters (springs). The thin segments behave as torsional springs when the resonator is clamped by the top and bottom. A sinusoidal current passing through a pair of coils drives a magnet in the resonator causing small torsional oscillations (0.001° maximum angular displacement). Changes in the positions and bandwidths of the five natural resonance frequencies for the device are determined as a function of reaction time or concentration of the solution surrounding the resonator. G' and G'' are determined from analysis of the resonance shifts and bandwidth broadening.

Immediately following mixing and complete homogenization of the reaction components, the solution was placed into the MLR and held at 30.000 °C for 15 to 45 minutes. After this equilibration period, data sets were collected continuously up to and through the macroscopic gel point. The MLR is enclosed to minimize solvent evaporation which may result in changes of the observed rheological properties.[34] The gelation point was taken as the time when a separate sealed aliquot of the reaction solution which was held at 30.000 °C did not flow upon inversion. These times were reproducible to within ±2% between runs. The gel times for the series of reactions under study are listed in Table I as a function of reaction solution pH. The time necessary to collect data for each set of five frequencies was less than 0.5% of the total duration of the reaction to gelation. Because of the small amplitude of the resonator motion in the MLR, the VE measurements on the reacting system are essentially performed without perturbation of the cluster growth and gel structure. No quenching of the polymerization reaction by temperature quench or catalyst poisoning was necessary for these measurements.

Results

Parts a and b of Figure 1 show measured values of log G' and log G'', respectively, as a function of reaction time t for a TEOS reaction with pH = 3.1. Data for each of the five MLR frequencies are shown for the entire reaction, with the exception that for the lowest resonance mode (104 Hz) even the sensitivity of the MLR was not sufficient to obtain G' values early in the reaction. The four higher frequency modes (431, 1060, 2600, 6200 Hz) each provide values for G' over the entire experiment duration. At very early times G' shows a rapid initial rise from below instrument resolution to the finite values shown in Figure 1a. This increase in G' is reproducible and presumably corresponds to the rapid initial growth of the polymer clusters which will eventually be linked into the three-dimensional network. After this initial rise log G' increases slowly with time during the first half of the reaction, but at a critical time, t_B, the slope in Figure 1a increases sharply. The corresponding change is not found in Figure 1b where a smooth transition of G'' through the region of t_B is observed. These general shapes of G' and G'' with time are similar to those observed for TEOS by Sacks and Sheu[35] using a concentric cylinder rheometer with a large angular displacement of 10° and a fixed frequency of 0.5 Hz. Sacks and Sheu have argued that the rapid increase in G' and G'' corresponds to the effect of extensive particle–particle interactions and network structure development.

We have determined an apparent break time, $t_B(\omega)$, by extrapolating the linear regions of log G' versus t to a crossover point as shown in Figure 1a. The value of t_B is frequency dependent with the break occurring first at the highest frequency and sequentially later for lower frequencies. Each experimental frequency probes the relaxation of the polymer solution on a length scale determined by the shear wavelength. For this viscoelastic solution the shear wavelengths[27] at the break are on the order of 1–100 μm, with the high frequencies measuring smaller distances than the low frequencies.

For reactions at higher pH no storage modulus was measurable before a time corresponding roughly to $t_B(\omega)$. Parts a and b of Figure 2 show the evolution of $G'(\omega)$ and $G''(\omega)$ for the pH = 4.4 reaction. The chemistry of the silicate reactions involves hydrolysis and subsequent monomer condensation, where the relative reaction rates depend in a complicated way on the catalysis conditions (pH), purity of reagents, temperature, and stoichiometry of reactants. Previous work has shown that for pH in the range 4–8 and for high water to TEOS ratios formation of highly branched silicate polymeric clusters is favored.[9,10] Compact, dense species (perhaps 10 nm in diameter) would exhibit little conformational dynamic elasticity until the reaction proceeds, and bonds are formed between clusters to produce much larger structures. The observation that the onset of a measurable dynamic elasticity occurs earliest at the highest frequencies might be explained in terms of cluster growth to a critical size governed by a frequency-dependent shear wavelength, as described above.

The macroscopic gel points listed in Table I for each set of reaction conditions were determined semiquantitatively by observation of flow on inversion of a sealed vial of solution. No readily observable change occurs in G' or G'' at these times. It has been suggested that for some polymers G' equals G'' at the gel point, independent of frequency.[6,36–38] Our data show the crossover of G' and G'' after the macroscopic gel point. Variations of observed gel times for reactions in different sized containers are not sufficient to account for this difference. The difference also persists for gels prepared at different pH's with both longer and shorter reaction times. The G' and G'' crossover data shows some frequency dependence, although the dependence is slight and may be ambiguous.

The processes of cluster growth and gelation are qual-

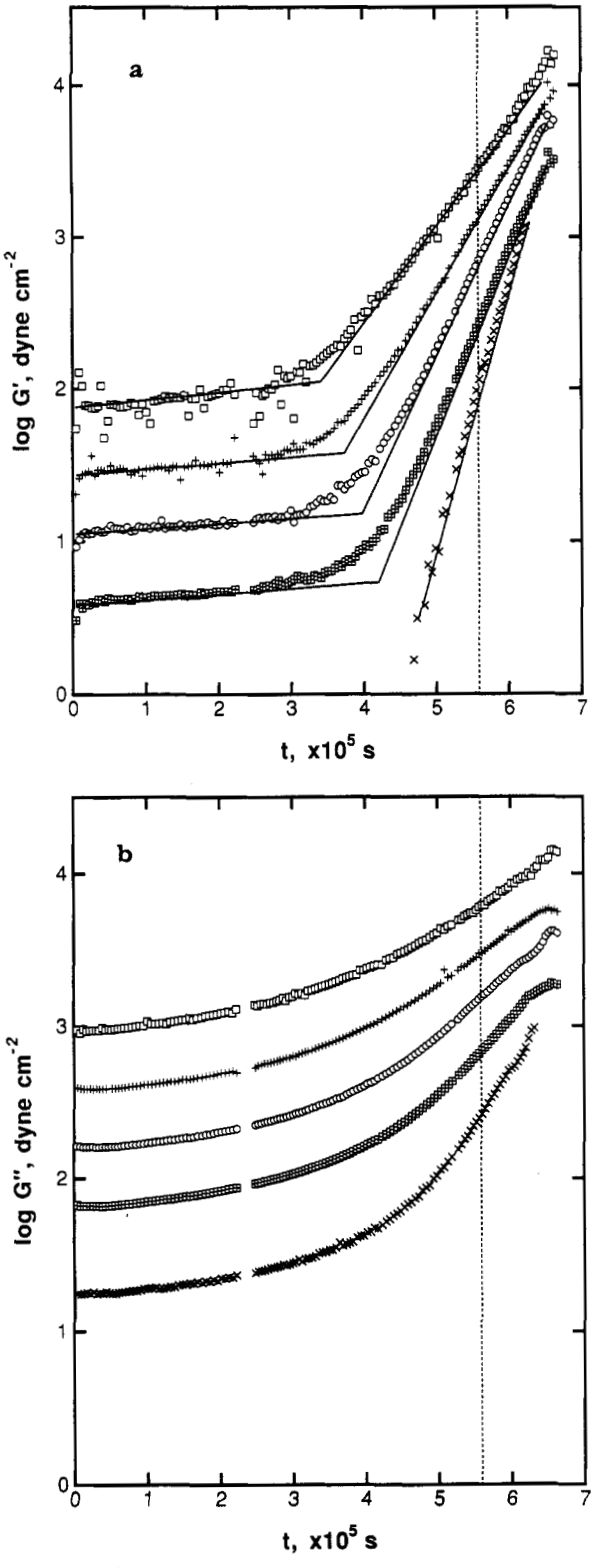

Figure 1. a. Change of dynamic storage moduli at five frequencies (×, 104, ⊞, 431, ○, 1060, +, 2600, □, 6200 Hz) with time for the pH = 3.1 TEOS reaction. Extrapolations show a frequency-dependent crossover in the modulus growth rate. Dashed vertical line indicates the time of the macroscopic gel point. b. Change in dynamic loss moduli at five frequencies (×, 104, ⊞, 431, ○, 1060, +, 2600, □, 6200 Hz) with time for the pH = 3.1 TEOS reaction. Dashed vertical line indicates the time of the macroscopic gel point.

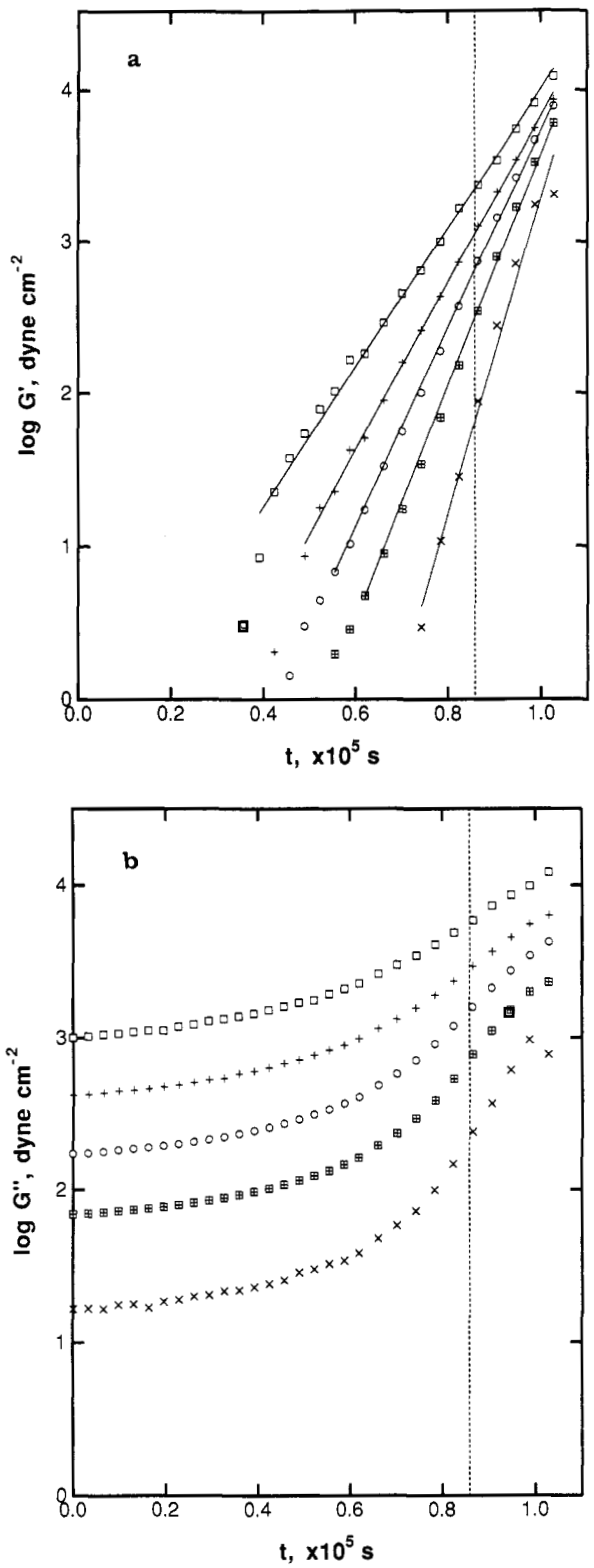

Figure 2. a. Change of dynamic storage moduli at five frequencies (×, 104, ⊞, 431, ○, 1060, +, 2600, □, 6200 Hz) with time for the pH = 4.4 TEOS reaction. Extrapolations show a frequency-dependent onset of measurable dynamic elasticity. Dashed vertical line indicates the time of the macroscopic gel point. b. Change in dynamic loss moduli at five frequencies (×, 104, ⊞, 431, ○, 1060, +, 2600, □ 6200 Hz) with time for the pH = 4.4 TEOS reaction. Dashed vertical line indicates the time of the macroscopic gel point.

itatively demonstrated in Figure 3 where the loss tangent, tan $\delta = G''/G'$, is shown as a function of time for five frequencies ranging from 104 to 6200 Hz for the pH = 3.1 reaction. For each frequency four regions along the reaction coordinate can be identified. An initial drop occurs in the beginning stage of the reaction corresponding to the initial rapid growth of clusters, which causes G' to become measurable. Next G' and G'' increase together, and the growing population of clusters results in a slight rise in tan δ. During this period it appears

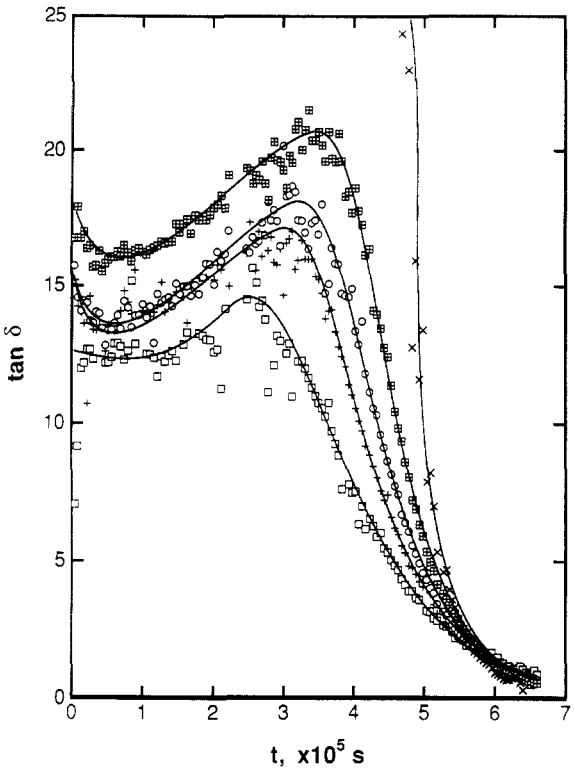

Figure 3. Viscoelastic loss tangent as a function of time for five frequencies as indicated in Figures 1 and 2. Lines are drawn to guide the eye.

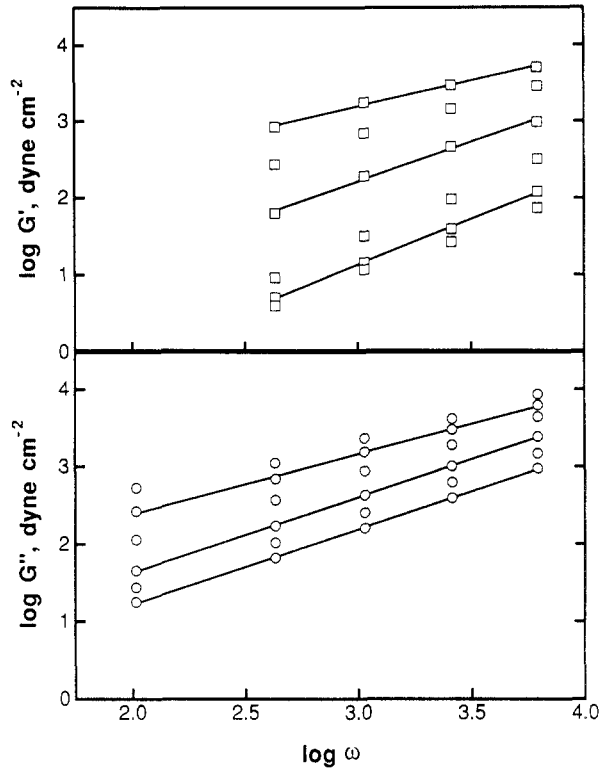

Figure 4. Double log plot of G' (□) and G'' (○) against measurement frequency at times of 30 000, 407 300, 503 800, 560 400, 600 500, and 651 900 s from the bottom to the top. Slopes yield the viscoelastic exponent Δ from eq 6.

that on the frequency scale of these measurements the clusters are not changing greatly. The growth phase continues until the tan δ values reach maxima at times near those identified in Figure 1a as t_B. From the maxima, tan δ has a rapid drop which emphasizes the growth of clusters beyond the spatial dimensions of the probing frequencies. The decrease continues until, following the formation of a macroscopic gel structure, tan δ passes through 1 as $G' = G''$ independent of frequency. The reaction time where tan $\delta = 1$ has been identified with the gelation time.[38] We observe that the gel point, determined as noted above by observation of the cessation of flow, occurs somewhat earlier.

Figure 4 shows log G' and log G'' against log ω for several measurement times along the reaction. The slopes of these lines yield Δ, the viscoelastic exponent from eq 6, for the frequency dependence of the moduli. The changes of Δ with extent of reaction can be seen in Figure 5 where Δ' and Δ'' for storage and loss moduli, respectively, are plotted against time. As noted in the introduction, values of Δ near the gelation critical point are predicted by the various theories. Early in the reaction the values are relatively constant at $\Delta' = 1.1$ and $\Delta'' = 0.95$ for the storage and loss moduli, respectively. At later times Δ' increases strongly to 1.3 while Δ'' increases only to 1.0. Both then decrease and merge (within experimental error) to 0.76 at about 575 000 s.

Previous work[17-19] concentrated on the limiting values of Δ. For the present experiments the limiting values are $\Delta' = 0.73$ and $\Delta'' = 0.71$. These values of Δ compare very well with the value noted earlier as a prediction based on the percolation model for dynamic moduli at the gel point with the assumption of Rouse dynamics[4,19] ($\Delta = {}^2/_3$) and also with the value of 0.72 ± 0.2 calculated from the s and t determined for superconductor–resistor networks. The limiting values are also in agreement with previously measured values for epoxy resins,[18] polyurethanes,[17] and polyesters.[19] The results are not

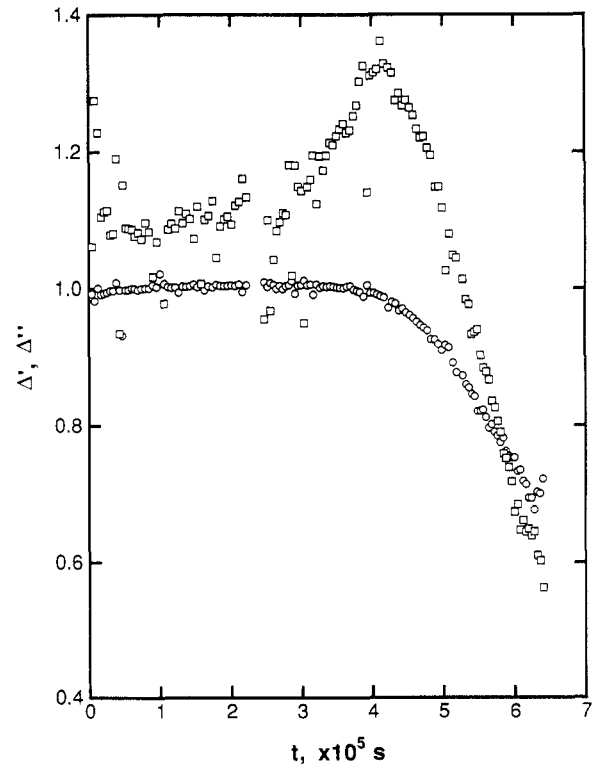

Figure 5. Changes of viscoelastic exponents for Δ' the storage (□) and Δ'' the loss (○) shear moduli during the course of the gelation reaction as obtained from fits such as those shown in Figure 4.

consistent with predictions of FS mean field theory[1,2,7] ($\Delta = 1$) or with experimental work for the cross-linking of PDMS with an excess of cross-linker[6] ($\Delta = {}^1/_2$). The limiting frequency behavior for the three reaction conditions is given in Table I.

Discussion

The existence of a measurable dynamic storage modulus during the entire reaction course points to the formation of polymeric clusters during the initial hydrolysis period, thereby creating a viscoelastic fluid. This seems to occur during the first 10% of the reaction time as is seen by the first few data points in Figure 1, where a rapid initial increase in G' is observed. Previous work with the MLR[39] suggests that for solutions of comparable viscosity linear polymer chains must be on the order of 30 000 molecular weight for the instrument to yield reproducible results.

In the percolation model the reaction bath consists of a self-similar distribution of noninteracting fractal clusters. Within the percolation model it is assumed that clusters of the same size are separated by a distance proportional to their radius and are therefore effectively prohibited from overlapping.[4,7,19] The gelation reaction proceeds simultaneously on all size scales; on the smallest scale clusters grow, increasing in size throughout the reaction as monomer continues to react and add to existing clusters. Simultaneously cluster–cluster aggregation occurs which ultimately leads to the formation of a macroscopic gel. Qualitatively, if the relaxation times of the clusters are faster than the time scale of the measurement (as set by the experimental frequency) gel behavior is not expected. As the reaction continues the relaxation time scale of the cluster population will diverge with very fast local relaxations and also much slower global relaxations. While the relaxations of the smallest species will always be much faster than the probe frequency, the presence and continuing growth of large clusters lead to a gel structure which exists on a spatial scale comparable to the shear wavelength (1–100 μm).[27] Thus the gel cluster is "macroscopic" to the higher frequencies while at lower frequencies the experiment continues to probe a distribution of clusters smaller than the length scale of the measurement.

As noted in the introduction the complex modulus is scaled by the changing steady-state creep compliance, J_e^0, during the process of gelation. In our experiment, where G' and G'' are measured at multiple-fixed frequencies as a function of reaction time, this is evidenced by a monotonic shift of modulus values to higher absolute magnitudes. At the same time the effective frequencies to which our experimentally fixed frequencies correspond must scale by the changing longest relaxation time, τ_z, of the solution. Together these two effects introduce horizontal and vertical shifts to the data. For this experiment we have no independent measurement of J_e^0 or τ_z, but they can be determined by applying vertical and horizontal shifts to individual data sets to produce a unique master curve.

Such a composite plot is shown in Figure 6 where the empirical horizontal and vertical shift factors are indicated by a_h and a_v, respectively. There is some uncertainity in performing these manipulations and with a more limited set of data it would be difficult to justify, but since both the slopes of G′ and G″ and their relative magnitudes are changing significantly throughout the course of the reaction (as is apparent from Figures 3 and 5) the requisite shift factors are not difficult to determine. This master curve includes data sets from over 45 time slices taken during the gelation reaction in the period from 2×10^5 to 6×10^5 s.

The reaction coordinate follows the increasing effective modulus and frequency as the data shifts from the lower left to the upper right. Data from earlier reaction times can also be reduced onto this curve, but the goal

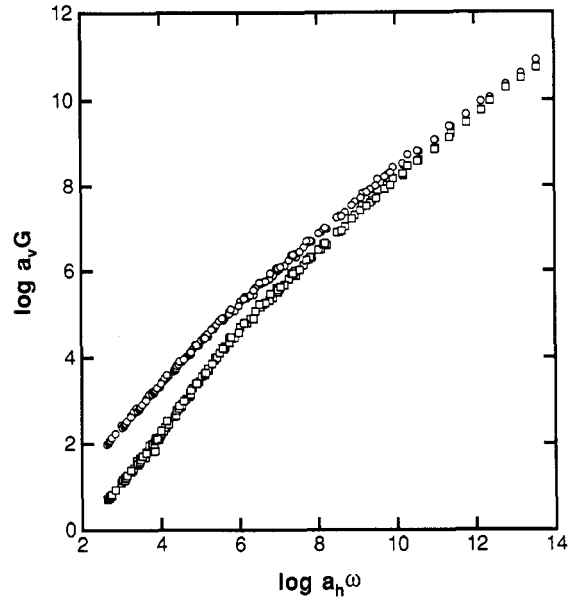

Figure 6. Composite plot of log G' (□) and log G'' (○) versus log effective frequency constructed from data sets at different points during the gelation reaction. The horizontal shift follows the longest relaxation time τ_z and the vertical shift corresponds to steady-state creep compliance J_e^0.

in producing the master plot is to acquire values for the vertical and horizontal shift factors as the critical point is approached. As noted above, a_v corresponds to J_e^0 and a_h follows τ_z. Equations 8 and 9 give the expected scaling relationships for these quantities with respect to extent of reaction under the percolation model for gelation near the critical point. Figure 7 shows the resulting log plot for a_h and a_v versus log ϵ, with $\epsilon = |t - t_c|/t_c$ where t is the reaction time and t_c is the time of gelation. As discussed above there is some ambiguity in picking a value for the gelation time. Some workers have suggested that t_c is best defined operationally as the value which yields clear scaling behavior near the critical point. This method for assigning t_c is very sensitive, and the values are found to lie between the times listed in Table I for the cessation of flow and those listed for G' equaling G''. Since the power law slopes in Figure 7 are sensitive to the choice of t_c, these three measures of gelation provide the error limits in determining the divergence exponents s and t. The values obtained for s and t are given in Table I, and even with the uncertainty in t_c the error bounds are comparable to those given by other workers. The third exponent in Table I, which is the ν from eq 1, is calculated from t as $\nu = t/d$ where d is the spatial dimensionality (=3).

Comparisons of the critical exponents in Table I for this series of experiments with those previously reported from theory and experiment shows good agreement. As noted above, Δ, the exponent for frequency dependence of the storage and loss shear moduli, agrees well with percolation predictions for either Rouse-like dynamics or computer simulations of resistor networks. Experimental values measured on epoxy resins, polyurethanes, and polyesters are also comparable.[17-19] For the experiments given in Table I, the exponent s takes values of $0.8_8 \pm 0.10$ which are close to the prediction of $s = 0.75 \pm 0.06$ given by the divergence of conductivity in a superconductor–resistor network,[25] and it falls within the broad range delimited by the Zimm and Rouse limits ($0 \leq s \leq 1.35$) for branched polymer structures.[4,19] Within experimental error s agrees with the experimental value $s = 1.1 \pm 0.3$ reported by Gauthier-Manuel et al.[26] for the

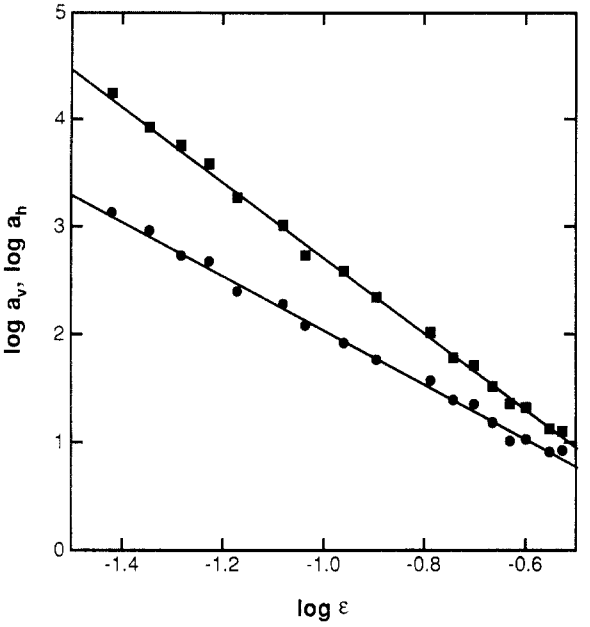

Figure 7. log-log scaling plot of a_h (■) and a_v (●) versus ϵ the reduced extent of reaction for the region approaching the gelation critical point. According to eqs 8 and 9 the slopes yield divergence exponents $-s-t$ and $-t$ for τ_z and J_e^0, respectively.

uncatalyzed gelation of tetramethoxysilane (TMOS). However, these results are lower than the values found for some other silica gel systems, where Colby et al.[40] found $s = 1.3 \pm 0.2$ and Martin et al.[15] found $s = 1.5 \pm 0.2$. The latter of these was from an interpretation of light scattering results. The difference is small, but significant in distinguishing the various theoretical developments. It could result from the use of TEOS instead of TMOS in the gelation reaction, or it might be the result of differences in the nature of the experimental technique (i.e., light scattering versus direct viscoelastic measurements). Another more interesting difference is that the previous experiments were performed on diluted samples while our measurements were taken on the actual reaction bath. Further studies are underway that will investigate these differences.

The measured value of $t = 2.4 \pm 0.2$ compares much better with the percolation value $t = 2.67$ for $d = 3$ than either the higher mean field prediction of $t = 3$ or the calculated value $t = 3.96 \pm 0.04$ for resistor networks.[24] On the other hand, Adam et al.[16] found $t = 3.2 \pm 0.5$ for a polycondensation reaction producing polyurethanes while $t = 3.6 \pm 0.4$ for TMOS.[26] The final column in Table I, the calculated values of ν, represents the scaling of the divergence of the cluster radius. It also agrees with the percolation theory prediction of 0.85 rather than the mean field prediction of 0.5.

Previous experiments performed on silica-based gelation systems have shown no significant dependence of scaling relationships on the catalyst used for the reaction.[9,10,15] This is also the case for this set of measurements where the acid concentration is varied by a factor of 20. The Δ, s, t, and ν exponents listed in Table I are within their experimental error limits. Only for s is there a systematic difference between the gels prepared at different pH values. Since this pH range represents nearly the entire limit of conditions which produce "clear" gels, the values given in Table I appear to provide a universal description for this class of TEOS gelation. Although the exponents reported here are in reasonable agreement with the predictions of percolation theory there remain discrepancies with some values previously reported for alkoxysilane gels.

There may be some differences in experimental measurement techniques or in reaction conditions, which can explain the differences, but one of the most disturbing sources for uncertainty in the exponents comes from the choice of the gelation time t_c. Our observation, made by substituting longer gelation times which are clearly beyond the observed gel formation, is that the power law behavior in Figure 7 was not compromised and the values of s and t continued to increase. This would put these exponents in better agreement with some of the previous results.

Conclusion

The qualitative observations from this study provide a reasonably consistent picture of the gelation reaction. The increase of both G' and G'' with time follows the growth of polymeric clusters throughout the course of the reaction. The observed frequency-dependent break in G' at a time t_B argues for the presence of clusters of increasing spatial dimension. Also observed is a shift of the effective frequency, based on the divergence of the longest relaxation, and of the modulus, due to divergence of the steady state shear compliance. A composite plot of dynamic storage and loss shear moduli versus effective frequency is constructed. All of the deduced divergence exponents are in reasonable agreement with the percolation model.

Experiments are in progress to further characterize the effects of reaction conditions on the TEOS gelation dynamics. Dynamic VE measurements on both acid- and base-catalyzed systems with high and low water contents will be performed to investigate the influence of different types of cluster growth. Of particular interest are high acidity/low water silica systems which should produce gels with long chains between cross-links. These can be compared to base-catalyzed systems which produce compact, highly cross-linked, colloidal gels. Studies of the frequency dependence of t_B and its relationship to the growth of the gel structure are also being performed. The MLR data will also be complemented by a combination of light scattering and NMR measurements which will independently characterize the dimensions of the growing clusters. Simultaneous determination of the divergences of static and dynamic properties should provide a powerful test of theoretical models and predictions for the gelation critical point phenomenon.

Acknowledgment. This work was supported by the National Science Foundation, Polymers Program (DMR-8715567), and by the Eastman Kodak Corp. We are grateful for useful suggestions from Drs. Ralph H. Colby, Michael Rubinstein, and Douglas Adolf.

References and Notes

(1) Flory, P. J. *J. Am. Chem. Soc.* **1941**, *63*, 3083.
(2) Stockmayer, W. H. *J. Chem. Phys.* **1943**, *11*, 45.
(3) Cates, M. E. *J. Phys. (Paris)* **1985**, *46*, 1059.
(4) Martin, J. E.; Adolf, D.; Wilcoxon, J. P. *Phys. Rev. A* **1989**, *39*, 1325.
(5) Muthukumar, M. *J. Chem. Phys.* **1985**, *83*, 3161.
(6) Hess, W.; Vilgis, T. A.; Winter, H. *Macromolecules* **1988**, *21*, 2356.
(7) Stauffer, D.; Coniglio, A.; Adam, M. *Adv. Polym. Sci.* **1982**, *44*, 103.
(8) de Gennes, P.-G. *Scaling Concepts in Polymer Physics*; Cornell University Press: Ithaca, NY, 1979.
(9) Schaefer, D. W.; Keefer, K. D. *Phys. Rev. Lett.* **1984**, *53*, 1383.
(10) Schaefer, D. W.; Keefer, K. D. In *Better Ceramics Through Chemistry I*; Brinker, C. J., Clark, D. E., Ulrich, D. R., Eds.; Mater. Res. Soc. Proc. 32; North-Holland: New York, 1984; p 1.

(11) Cabane, B.; Dubois, M.; Duplessix, R. *J. Phys. (Paris)* **1987**, *48*, 2131.
(12) Martin, J. E.; Keefer, K. D. *Phys. Rev. A* **1986**, *34*, 4988.
(13) Martin, J. E.; Wilcoxon, J.; Adolf, D. *Phys. Rev. A* **1987**, *36*, 1803.
(14) Patton, E. V.; Wesson, J. A.; Rubinstein, M.; Wilson, J. C.; Oppenheimer, L. E. *Macromolecules* **1989**, *22*, 1946.
(15) Martin, J. E.; Wilcoxon, J. P. *Phys. Rev. Lett.* **1988**, *61*, 373.
(16) Adam, M.; Delsanti, M.; Durand, D. *Macromolecules* **1985**, *18*, 2285.
(17) Durand, D.; Delsanti, M.; Adam, M.; Luck, J. M. *Europhys. Lett.* **1987**, *3*, 297.
(18) Martin, J. E.; Adolf, D.; Wilcoxon, J. P. *Phys. Rev. Lett.* **1988**, *61*, 2620.
(19) Rubinstein, M.; Colby, R. H.; Gillmor, J. R. *Polym. Prepr. (Am. Chem. Soc., Div. Polym. Chem.)* **1989**, *30* (1), 81.
(20) Ulrich, D. R. *J. Non-Cryst. Sol.* **1988**, *100*, 174.
(21) Bechtold, M. F.; Mahler, W.; Schunn, R. A. *J. Polym. Sci., Polym. Chem. Ed.* **1980**, *18*, 3623.
(22) Adam, M.; Delsanti, M.; Munch, J. P.; Durand, D. *J. Phys. (Paris)* **1987**, *48*, 1809.
(23) de Gennes, P.-G. *C. R. Acad. Sci., Ser. B* **1978**, *286*, 131.
(24) Zabolinski, J. G.; Bergman, D. J.; Stauffer, D. *J. Stat. Phys.* **1986**, *44*, 211.
(25) Herrmann, H. J.; Derrida, B.; Vannimenus, J. *Phys. Rev. B* **1984**, *30*, 4080.
(26) Gauthier-Manuel, B.; Guyon, E.; Roux, S.; Gits, S.; Lefaucheux, F. *J. Phys. (Paris)* **1987**, *48*, 869.
(27) Ferry, J. D. *Viscoelastic Properties of Polymers*; John Wiley and Sons: New York, 1980.
(28) Hair, D. W.; Niertit, F. J.; Hodgson, D. F.; Amis, E. J. *Rev. Sci. Instrum.* **1989**, *60*, 2780.
(29) Schrag, J. L.; Johnson, R. M. *Rev. Sci. Instrum.* **1971**, *42*, 224.
(30) Hair, D. W.; Amis, E. J. *Macromolecules* **1989**, *22*, 4528.
(31) Keefer, K. D. In *Better Ceramics Through Chemistry I*; Brinker, C. J., Clark, D. E., Ulrich, D. R., Eds.; Mater. Res. Soc. Proc. 32; North-Holland: New York, 1984; p 15.
(32) Schaefer, D. W.; Keefer, K. D. In *Better Ceramics Through Chemistry II*; Brinker, C. J., Clark, D. E., Ulrich, D. R., Eds.; Mater. Res. Soc. Proc. 73; North-Holland: New York, 1986; p 277.
(33) Bailey, J. K.; Mecartney, M. L. In *Better Ceramics Through Chemistry III*; Brinker, C. J., Clark, D. E., Ulrich, D. R., Eds.; Mater. Res. Soc. Proc. 121; North-Holland: New York, 1988; p 367.
(34) Kozuka, H.; Kuroki, H.; Sakka, S. *J. Non-Cryst. Sol.* **1988**, *100*, 226.
(35) Sacks, M. D.; Sheu, R.-S. *J. Non-Cryst. Sol.* **1987**, *92*, 383.
(36) Winter, H.; Chambon, F. *J. Rheol.* **1986**, *30*, 367; **1987**, *31*, 683.
(37) Chambon, F.; Winter, H. *Polym. Bull.* **1985**, *13*, 499.
(38) Holly, E. E.; Venktaraman, S. K.; Chambon, F.; Winter, H. H. *J. Non-Newtonian Fluid Mech.* **1988**, *13*, 17.
(39) Hodgson, D. F.; Hair, D. W.; Amis, E. J. Unpublished results.
(40) Colby, R. H.; Coltrain, B. K.; Salva, J. M.; Melpolder, S. M. In *Fractal Aspects of Materials: Disordered Systems*; Hurd, A. J., Weitz, D. A., Mandelbot, B. B., Eds.; Materials Research Society: Pittsburgh, 1987.

Molecular Structures and Solution Viscosities of Ethylene–Propylene Copolymers

Ashish Sen and Isaac D. Rubin*

Texaco Research Center, P.O. Box 509, Beacon, New York 12508. *Received August 10, 1989; Revised Manuscript Received November 15, 1989*

ABSTRACT: Dilute solution studies on ethylene–propylene (EP) copolymers in hydrocarbon solvents at −10 to +50 °C showed that highest viscosities were obtained in methylcyclohexane and lowest in toluene and tetralin (tetrahydronaphthalene). The copolymers contained 58–80 mol % ethylene; their $\bar{M}_w$ values were 148 000 to 322 000 and only those with 80% ethylene contained crystallinity. The solvating power of aliphatic solvents for amorphous copolymers, as measured by viscosity, decreased slowly with rise in temperature while that of the aromatics improved slightly to 20 °C and then remained constant or gradually diminished. The low-temperature solubility of partially crystalline copolymers was poorer in most solvents, improved rapidly to 20 °C, and then changed little with temperature. Linear double logarithmic plots of $[\eta]$ against $\bar{M}_w$ were obtained for all EPs in methylcyclohexane, but the Mark–Houwink equation did not describe low-temperature data in toluene. Equivalent hydrodynamic volumes were calculated. Behavior of partially crystalline copolymers in poor solvents at low temperatures is explained by ordering of the longer ethylene sequences into aggregates or partially ordered domains.

Introduction

There are only scattered reports in the literature on dilute solution properties of ethylene–propylene copolymers[1–8] and just a few of them address the effect of temperature on solution behavior.[5–8] This is rather surprising in view of the extensive commercial applications of EP copolymers. One of their important applications is in motor oils where they modify the viscosities of the oils and extend the temperature range over which they can be used. The purpose of our work is to gain a better picture of polymer–solvent interactions of EP copolymers in hydrocarbon solvents and increase our understanding of their behavior in the temperature range useful for motor oils. With this in mind, we investigated the effect of aliphatic and aromatic hydrocarbon solvents on the solution viscosity of EP copolymers in the temperature range of −10 to +50 °C using five copolymers differing in such key properties as molecular weight, ethylene to propylene ratio, length of ethylene sequences, and crystallinity.

Experimental Section

The ethylene–propylene copolymers were prepared with a soluble Ziegler–Natta catalyst composed of an alkylaluminum halide and a vanadium salt. Molecular weights and polydispersity were obtained by means of gel permeation chromatography (GPC) in 1,2,4-trichlorobenzene at 135 °C utilizing a Waters 150 C

* To whom correspondence should be addressed.

0024-9297/90/2223-2519$02.50/0